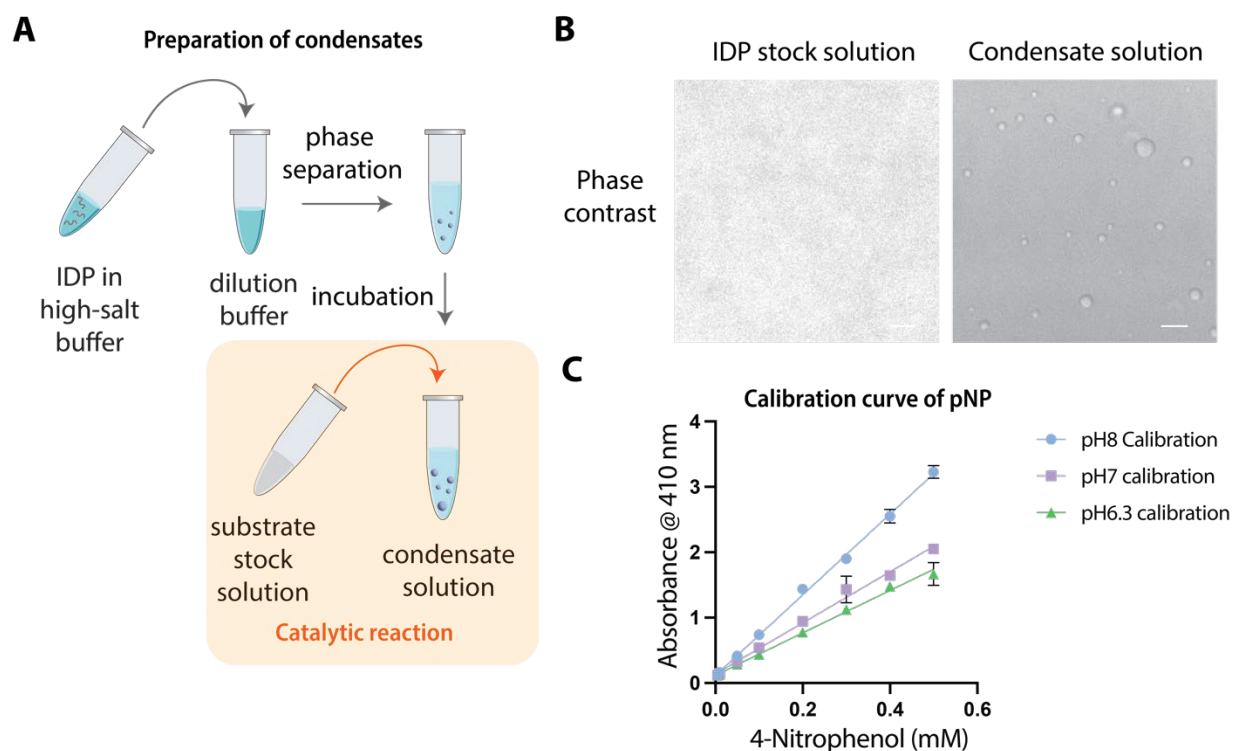


## Supplementary Figures



**Figure S1. Phase separation assay and calibration.**

**A**, Purified IDP is stored in a high-salt buffer, in which the protein remains soluble. The protein stock solution is added into a dilution buffer to trigger phase separation and the solution is incubated at room temperature for 30 min to allow condensate formation. For catalytic reaction, a high-concentration substrate stock solution is added into the condensate solution in a volume ratio of 1:200 to minimize the effects of the substrate solvent (e.g., acetonitrile) on condensate stability.

**B**, Representative phase contrast images of IDP stock solution and condensate solution. Scale bar is 10  $\mu\text{m}$ .

**C**, Calibration curves of the concentration of the reaction product (p-nitrophenol) and the optical absorbance at 410 nm was constructed based on different buffer conditions. These buffer conditions cover the testing conditions in this study.

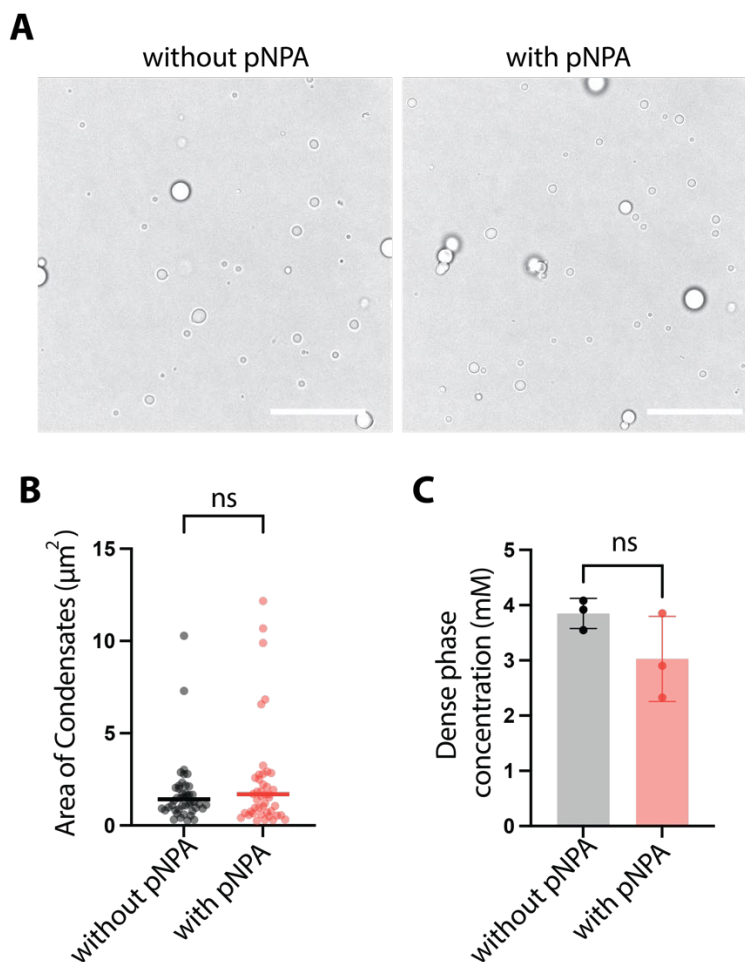
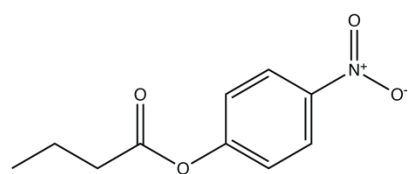


**Figure S2. Characterization of condensates with or without the addition of pNPA.**

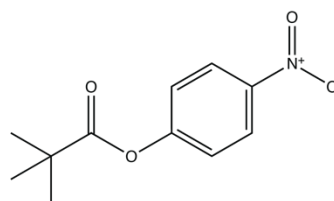
**A**, Bright-field confocal images of RLP<sub>WT</sub> condensate samples with or without the addition of pNPA incubated for the same amount of time (120 min). For the sample without the addition of pNPA, same volume of acetonitrile was added, which is the solvent of the pNPA stock solution. Scale bar is 20  $\mu\text{m}$ .

**B**, Quantification of the areas of individual condensates resided on the cover glass. ns, non-significant based on unpaired t-test with  $p=0.1057$ .  $N=50$ .

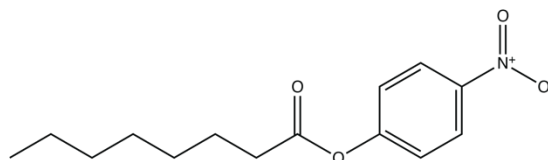
**C**, Sedimentation assay quantification of the dense phase concentration of the RLP<sub>WT</sub> condensate samples with or without the addition of pNPA. The condensate solution was dialyzed against the same reaction buffer without pNPA to remove the reactants and the products before subjecting the samples to sedimentation assay. ns, non-significant based on unpaired t-test with  $p=0.1587$ .  $N=3$ .



4-nitrophenyl butyrate



4-nitrophenyl trimethylacetate



4-nitrophenyl octanoate

**Figure S3. Evaluation of catalytic specificity of condensates using different nitrophenyl ester substrates with distinct side-chains.**

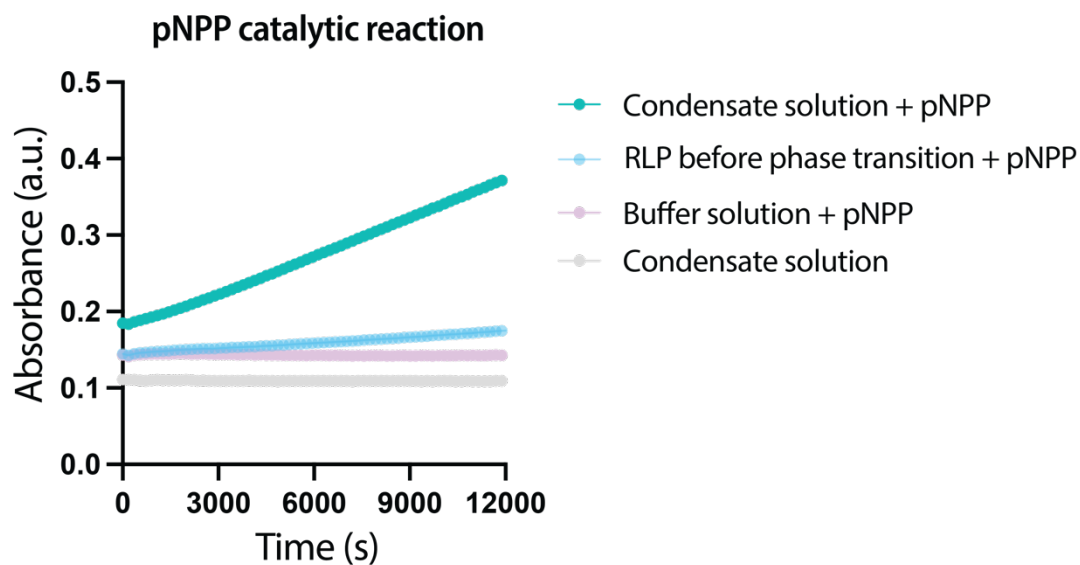


**Figure S4. Catalytic assay of p-nitrophenol phosphate.** 5 mM p-nitrophenol phosphate (pNPP) was added into solutions with condensates (30  $\mu$ M RLP<sub>WT</sub>), with RLP<sub>WT</sub> protein before phase transition (20  $\mu$ M RLP<sub>WT</sub>) and without proteins. A control with only condensate solution was used to evaluate the background signal.

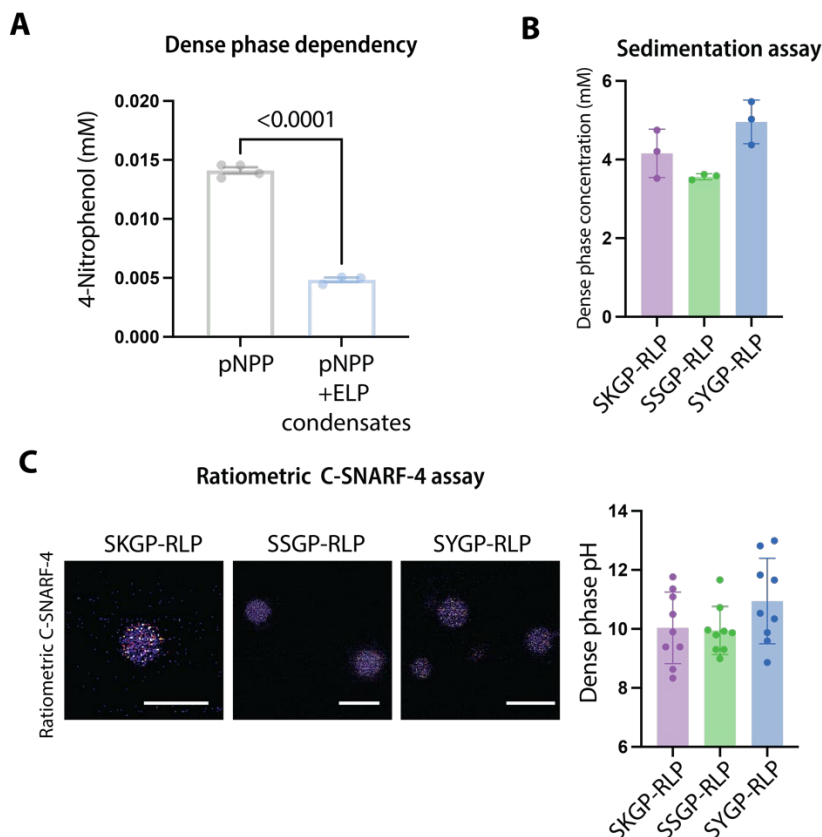


### Figure S5. Decoupling the factors that contribute to the catalytic functions.

**A**, Analysis of the capability of ELP condensates on driving the decomposition of p-nitrophenol phosphate through evaluating the concentration of 4-nitrophenol after 4 h of incubation of pNPP with ELP condensates at room temperature. Interestingly, the ELP condensates inhibited the decomposition of pNPP. This observation suggests that the hydrophobic nature of ELP interior environments might prevent the solvation of the pNPP into the condensates, thereby creating some “exclusion” zones to prevent pNPP from decomposition by water molecules.

**B**, Condensates were incubated for 2 h at room temperature before conducting the following characterizations. Sedimentation assay for the evaluation of the dense phase concentration of condensates formed by RLP sequences containing different N-terminus sequences. Compared between sequences, a slightly higher dense phase concentration was observed in the condensates formed by SYGP-RLP. This observation is explained by the mutation from Lys to Tyr in the N-terminus sequence, which should mediate a stronger dense phase interactions. N=3 independent experiment.

**C**, C-SNARF-4 assay for the evaluation of interior condensate pH formed by different sequences. No significant difference between each sequence was observed. This observation supports that the main sequence of RLP ([GRGDSPYS]<sub>20</sub>) determines the dense phase pH of condensates. N>8 global analysis of individual ratiometric images.

### Catalytic behaviors of native condensates

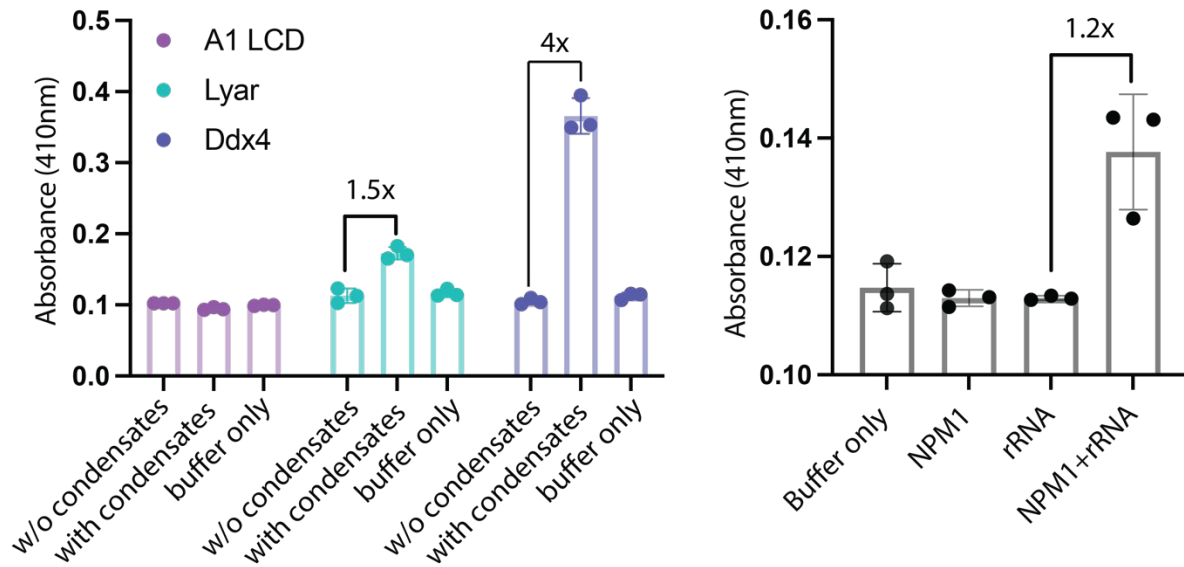


**Figure S6. Evaluation of the hydrolysis of pNPP by different condensates formed by native IDPs and complex coacervation between NPM1 and rRNA.** The hydrolysis reaction was conducted with 4 mM pNPP at 30 °C for 150 min. For condensates formed by IDPs only, the catalytic performance was compared between solutions containing IDP below  $C_{sat}$ , condensates and buffer only. For condensates formed by complex coacervation between NPM1 and rRNA, the catalytic performance was compared between solutions containing NPM1, rRNA, condensates by NPM1 and rRNA and buffer only.

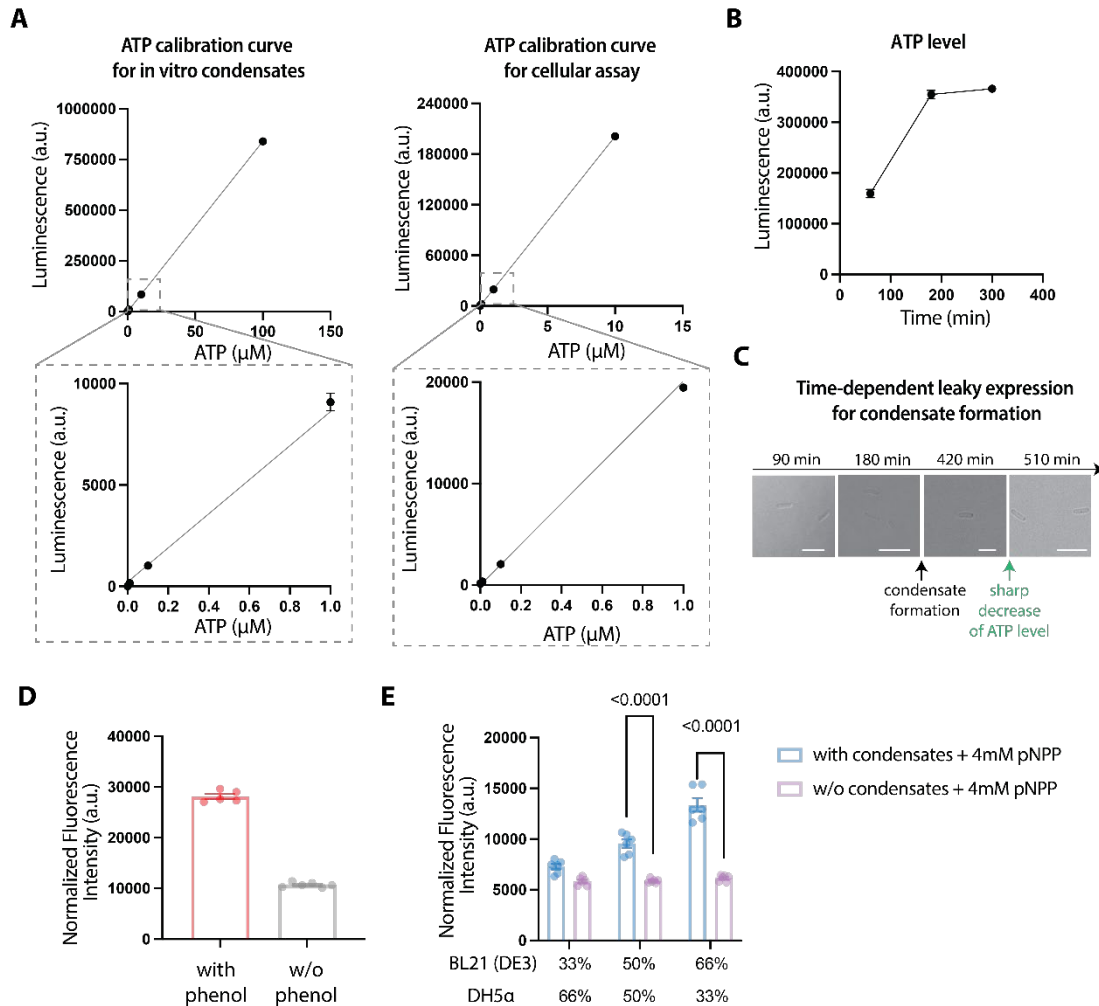


**Figure S7. Evaluation of the effects of condensate on the intracellular ATP level and the performance of intracellular gene circuits.**

**A**, ATP calibration curve constructed in the condensate formation buffer and the cellular assay buffer.

**B**, Evaluation of the effects of gene overexpression on the level of cellular ATP. The overexpression was induced by 0.5 mM IPTG at time zero.

**C**, Confocal images of phase contrast images of cells containing the plasmid encoding RLP<sub>WT</sub> regulated by a leaky T7 promoter. Without induction, condensate formation was observed at around 7 h, after which a sharp decrease of intracellular ATP level was observed as shown in Figure 5e.

**D**, Comparison of the normalized GFP signal of cells with DmpR circuit with or without the addition of 100  $\mu\text{M}$  of 4-nitrophenol after incubating for 24 h.

**E**, Comparison of normalized GFP signal of a cell population containing different fractions of the BL21 (DE3) (with the condensate circuit) and DH5 $\alpha$  (with the DmpR circuit) with the addition of 4

mM p-nitrophenol phosphate based on the conditions with or without condensates.  $P < 0.0001$  based on unpaired t-test.  $N=6$ .